ACS EARTH AND SPACE CHEMISTRY

Article

Cite This: ACS Earth Space Chem. 2018, 2, 634−639

Effect of Particle Morphology on Cloud Condensation Nuclei Activity

Muhammad Bilal Altaf,[†] Dabrina D. Dutcher,[‡,§] Timothy M. Raymond,[§] and Miriam Arak Freedman*[,†]

[†]Department of Chemistry, The Pennsylvania State University, University Park, Pennsylvania 16802, United States

[‡]Department of Chemistry and [§]Department of Chemical Engineering, Bucknell University, Lewisburg, Pennsylvania 17837, United States

Supporting Information

ABSTRACT: Cloud condensation nuclei (CCN) activation is sensitive to the size, composition, and morphology of aerosol particles of <200 nm. By controlling the particle morphology of internally mixed samples (i.e., homogeneous versus phase separated), we have probed the effect of morphology on CCN activity using model organic aerosol systems, where ammonium sulfate was mixed with either pimelic acid or succinic acid in a 50:50 mixture by weight. Surprisingly, for systems of the same composition but distinct morphology, we observe a noticeable impact on CCN activity. Specifically, a phase-separated morphology results in activation diameters close to that of ammonium sulfate, while a homogeneous morphology yields an activation diameter in between the pure inorganic and organic components. Our results suggest that morphology-resolved CCN data may be an important parameter to consider in cloud microphysics models to improve predictions of CCN activity of complex organic aerosols. For laboratory CCN studies, it is important to control or account for atomized solution drying rates, which have been shown to affect morphology and ultimately CCN activity.

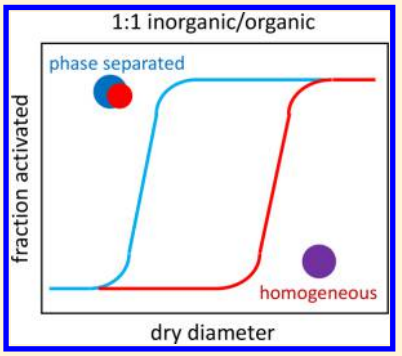

KEYWORDS: *liquid−liquid phase separation, organic aerosol, droplet activation, cloud microphysics, climate*

INTRODUCTION

Organic aerosol particles are chemically complex and ubiquitous in the Earth's atmosphere. Recently, a central focus of the atmospheric science community has been to understand the climate-forcing effects of these complex systems. For example, the impact of the aerosol indirect effect [i.e., the ability of aerosol particles to serve as cloud condensation nuclei (CCN)] on climate forcing remains highly uncertain.[1,2] It is essential to obtain a clear understanding of the population of aerosol that serves as CCN, because CCN play a critical role in cloud formation, lifetime, reflectivity, and precipitation.[1−4]

The tendency of an aerosol particle toward activation and growth via condensation to ultimately form a cloud droplet is controlled by a number of chemical and physical properties of the particle. Aerosol particle size and composition are key parameters in CCN activation that have received increasing attention in the literature.[1−4] The abilities of species, such as sulfates and abundant inorganic salts, to serve as CCN are relatively well-understood.[1,2] However, our understanding of the ability of organics to serve as CCN is quite limited and has resulted in a large uncertainty in the global modeling of cloud droplet nucleation and indirect forcing.[1] Recently, within the atmospheric chemistry community, interest has emerged in investigating the role of the particle mixing state and surface active organics on CCN activity.[5−7]

To better constrain the component of the indirect effect that is related to CCN, global models must represent the complexity of organic species and the degree of mixing of individual species with a given mass or size.[8] Thus, studies of parameters, such as particle morphology, which involve understanding the physics and chemistry of aerosol particles are critical. Recently, a number of studies have addressed the uncertainty that remains in the factors that contribute to hygroscopic growth and CCN activation in mixed particles.[5,9] The impact of the presence of liquid−liquid phase separation (LLPS) and the role of surface tension on the mechanism of cloud droplet formation and observed hygroscopicity parameters have received great interest as a result of their importance for our ability to predict cloud properties.[5,10−12] As shown in our previous work for systems that undergo LLPS, we have observed a size-dependent morphology of organic aerosol, where small particles are homogeneous and large particles are phase-separated.[13] We have also shown that, for some of the systems that we have explored, particle morphology can be controlled by varying the drying rate that particles experience in a given experiment.[14] Furthermore, we have previously demonstrated that, for a given system, phase-separated and homogeneous particles are mainly spherical in shape and have the same composition.[15]

In this work, we apply our results from earlier experiments that allow us to control particle morphology for model organic aerosol systems.[14] With the capabilities of the cloud condensation nuclei counter (CCNC) in mind, we designed

Received: December 15, 2017
Revised: April 30, 2018
Accepted: May 2, 2018
Published: May 2, 2018

DOI: 10.1021/acsearthspacechem.7b00146
ACS Earth Space Chem. 2018, 2, 634−639

a study to probe the effect of particle morphology on CCN activity. Specifically, we have worked with ammonium sulfate mixed with either pimelic acid or succinic acid and have investigated whether the morphology of a given system (i.e., phase separated versus homogeneous) impacts its CCN activity.

EXPERIMENTAL METHODS

Solution Preparation and Aerosol Particle Generation. Aerosol particles composed of ammonium sulfate (>99.0%, EMD), pimelic acid (>98%, Acros Organics), or succinic acid (>99%, Sigma-Aldrich) were generated from aqueous solution. Solutions for mixtures of each organic compound mixed with ammonium sulfate (at a 50:50 mass fraction) were also prepared. The concentrations of the aqueous solutions (prepared using high-performance-liquid-chromatography-grade ultrapure water) ranged from 0.05 to 0.3 wt % solute. Aerosol particles were generated at a high relative humidity (RH $\geq$ 96%) and a temperature of 295 K from the aqueous solutions using a constant output atomizer (TSI 3076, Shoreview, MN, U.S.A.). Nitrogen flow through the atomizer was approximately 1.5 L/min.

Controlling Particle Morphology. As discussed in our previous work, we are able to control particle morphology for the systems described above by altering the drying rates that particles experience in a given experiment.[14] To obtain a homogeneous morphology in the ~50−100 nm size regime, we use a diffusion dryer filled with molecular sieves (13× mesh size, Sigma-Aldrich; drying rate of 87.2% RH/s). Note that details of the calculation of drying rates are included in our previous work.[14] As we have shown previously, all of the particles in the size regime of interest (50−100 nm) are homogeneous when this drying rate is used.[14] A Tedlar bag (New Star Environmental, Roswell, GA, U.S.A.) can be used to slow down the drying rate by several orders of magnitude to 0.08% RH/s. This slower drying rate yields phase-separated (partially engulfed morphology) particles in the ~50−100 nm size regime. Note that all of the particles in this size regime have a partially engulfed morphology when this drying rate is used.[14,16] Thus, by employing this method, we can effectively control the morphology of particles used in our CCN studies.

Measuring CCN Concentrations. As seen in Figure 1, once the aerosol particles are generated and undergo drying, we can size select the aerosol stream using a differential mobility analyzer (DMA). The distribution of particle sizes exiting the DMA is determined by the theoretical transfer function when the particles are spherical.[17,18] On the basis of prior studies, we expect that ammonium sulfate, succinic acid, pimelic acid, and homogeneous particles composed of ammonium sulfate mixed with either organic acid are nearly spherical.[16] The phase-separated particles will have a more varied but still nearly spherical shape, with some deviation toward an elliptical shape.[16] We have shown, using a variety of mineral dust aerosol systems that the greater the deviation from a spherical shape, the greater the polydispersity of diameters transmitted through the DMA compared to the theoretical transfer function.[19−21] As a result, we expect that the transfer function for the phase-separated particles will be slightly more polydisperse than predicted by the theoretical transfer function. After size selection, the aerosol flow is split between a CCNC and a condensation particle counter (CPC). The detailed design and operation of the Droplet Measurement Technologies-CCNC (DMT-CCNC, Longmont, CO, U.S.A.) have been previously published.[22] Note that the particles are dry when they enter the CCNC. As shown in Figure 1, a CPC is included in the experimental setup to determine the concentration of particles. With this information, the fraction of particles activated as CCN can be determined as a function of the particle size.

Before investigation of the CCN activity of organic aerosol mixtures, the CCNC instrument was calibrated with ammonium sulfate, a system that has been well-characterized in the literature.[3] In each calibration experiment, four different temperature gradient values (ΔT) were used to check the linearity between critical supersaturation and temperature gradient. A large deviation from linearity indicates possible malfunction in the instrument, such as a faulty humidifier. Our experiments resulted in a linear calibration curve between the supersaturation and temperature gradient and, thus, did not indicate any issues with the operation of the instrument.

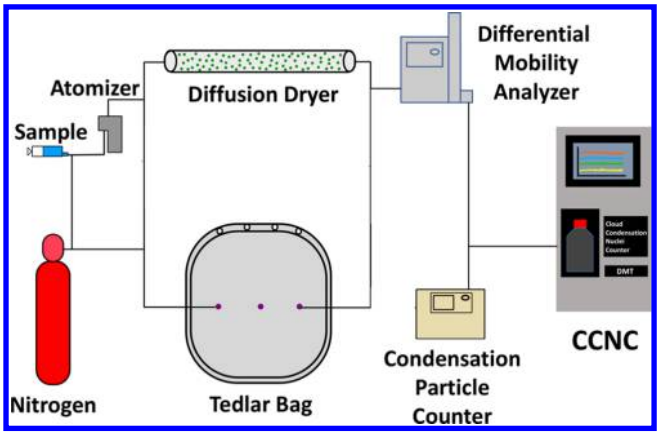

Figure 1. Schematic of the CCNC experiments. The aerosol flow either goes through the diffusion dryer or the bag, depending upon the desired drying rate.

RESULTS AND DISCUSSION

For the ammonium sulfate CCN experiments, 30 different dry diameter (Dp) values were size-selected by the DMA in the range of 15−220 nm. We note that we employed this method rather than scanning a range of particle diameters to allow for increased averaging time and adjustment for the particle concentration as the diameter changed. At each Dp, the total number concentration of aerosol particles, C_{CN}, was measured with a CPC. The number concentration of CCN, C_{CCN}, was measured with the CCNC. When these measurements were combined, the CCN efficiency (activated particle fraction, C_{CCN}/C_{CN}) was calculated from the averaged concentrations and a CCN efficiency spectrum of the fraction activated versus Dp was plotted. The CCN efficiency spectrum for ammonium sulfate at a 0.35% supersaturation is shown in Figure 2. Multiply charged particles can cause activation spectra to show a plateau before exponential growth phase of the curve. Rather than using any of the available charge correction algorithms, the data from these extraneous plateaus were eliminated from the data used for the sigmoid fits. The points not included in the regression data are shown using an alternate data marker, "×", in the spectra of the pure compounds. Using uncorrected data could result in a slight shift of the curve toward smaller particles (a leftward shift). It should also be noted that data significantly larger than the activation diameter were eliminated from the fit data as a common procedure.[23,24] When the standard error of

DOI: 10.1021/acsearthspacechem.7b00146
ACS Earth Space Chem. 2018, 2, 634−639

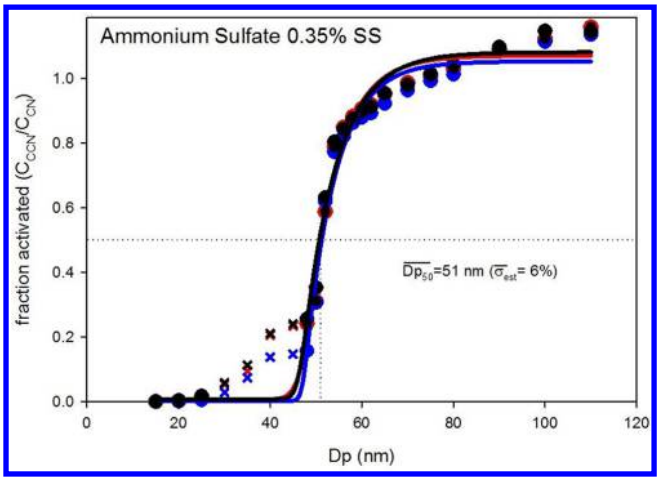

Figure 2. CCN efficiency spectra for ammonium sulfate. The circles represent raw data used for fitting the sigmoidal curve, while the "×" symbols represent data points from doubly charged particles, which were removed before fitting the curve but shown for completeness. The three colors represent different trials of the same system.

estimate from the regressions is used to calculate a 95% confidence interval for the activation diameter (Dp_{50}) of the ammonium sulfate, it contains the literature value at this supersaturation, which validates the regressions.

Sigmoid fits were calculated using SigmaPlot's (Systat Software, Inc.) dynamic curve fitting function with a five-parameter model. Equation 1 shows the form of the calculated regression:

$$f = y_0 + \frac{a}{\left(1 + \exp\left(-\frac{x - x_0}{b}\right)\right)^c} \quad (1)$$

where a, b, c, x_0, and y_0 are regression variables, f is the fraction of particles activated (C_{CCN}/C_{CN}), and x is the dry particle size, Dp (nm). Coefficients of determination for all reported fits were 0.97 or greater.

The collected data are corrected for doubly charged particles and fit with the sigmoid function described in eq 1. Figure 2 illustrates this process for ammonium sulfate, where the closed symbols represent the raw CCN data, the "×" symbols represent the data not included in the fit, and the solid lines depict the sigmoid fit to the experimental data, which is used to derive the activation diameter, Dp_{50}, where 50% of particles activate as CCN. We note that Figure 2 shows the CCN spectra and sigmoid fit for each individual trial. Dp_{50} is derived for each trial, and the average Dp_{50} is reported within the figure. We have obtained a Dp_{50} = 51 (nm) ± 6% for ammonium sulfate, in which the 95% confidence interval includes the literature value of 58 nm at a 0.35% supersaturation.[25,26] Note that, when multiple supersaturations are used, it is useful to calculate a κ factor to compare the hygroscopicities of different systems.[27] Because we have used only one supersaturation, we report only Dp_{50}.

Following the ammonium sulfate experiments, the CCN activity of the pure organic compounds, pimelic acid and succinic acid, was investigated at a supersaturation of 0.35%. Pimelic acid has an activation diameter of 70 nm (σ_{est} = 7%), while Dp_{50} = 58 nm (σ_{est} = 4%) for succinic acid. Figure 3 summarizes the CCN data for the pure organic compounds.

Because the goal of this work was to probe the effect of particle morphology on CCN activity, particles were generated

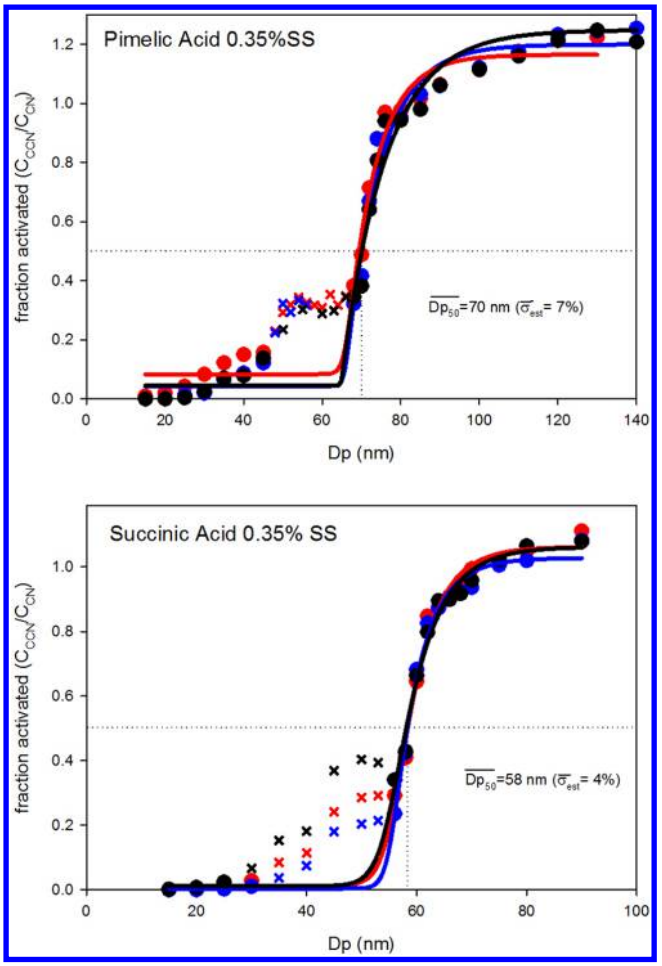

Figure 3. CCN efficiency spectra for pimelic acid and succinic acid. The circles represent raw data used for fitting the sigmoidal curve, while the "×" symbols represent data points from doubly charged particles, which were removed before fitting the curve but shown for completeness. The three colors represent different trials of the same system.

from 50:50 mixtures by weight of each organic compound and ammonium sulfate and measured in the CCNC. By controlling the particle drying rate for a given system, either a homogeneous or phase-separated morphology was obtained and investigated with the CCNC. We note that, as shown in our earlier work, 50:50 mixtures of ammonium sulfate mixed with either pimelic acid or succinic acid yield a partially engulfed morphology upon phase separation.[13] A phase-separated morphology for the 50:50 ammonium sulfate/pimelic acid system yielded an activation diameter of Dp_{50} = 52 nm (σ_{est} = 7%); however, for the same system, a homogeneous morphology resulted in a Dp_{50} = 58 nm (σ_{est} = 7%). Figure 4 summarizes the CCN spectra for ammonium sulfate, pimelic acid, and the 50:50 ammonium sulfate/pimelic acid system dried using a Tedlar bag (TB, phase-separated morphology) and diffusion dryer (DD, homogeneous morphology). We note that the summary spectra shown in Figure 4 are an average of multiple runs for each respective system. The individual data set for each trial is provided in Figure S1 of the Supporting Information. For Figures 2 and 3 and Figures S1 and S2 of the Supporting Information, individual data sets are fit to find individual Dp_{50} values, which are then averaged; for Figures 4 and 5, individual data sets are combined and then fit to find

DOI: 10.1021/acsearthspacechem.7b00146
ACS Earth Space Chem. 2018, 2, 634−639

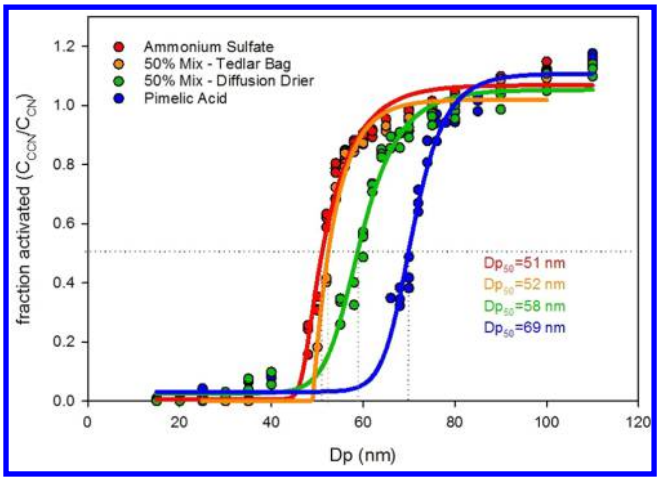

Figure 4. Summary CCN spectra for ammonium sulfate, pimelic acid, and the 50:50 ammonium sulfate/pimelic acid system dried using a TB (phase-separated morphology) and DD (homogeneous morphology).

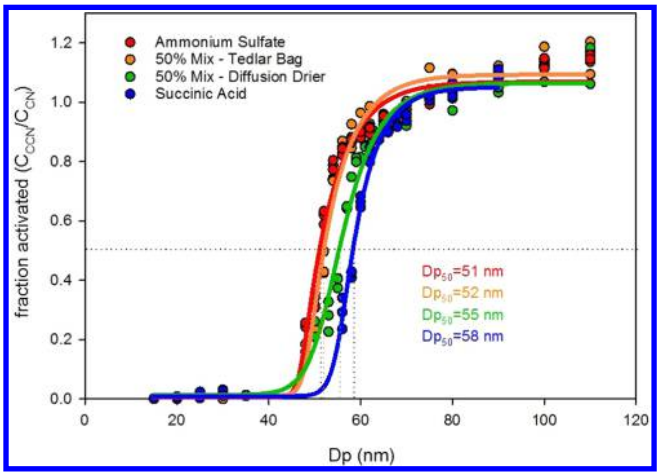

Figure 5. Summary CCN spectra for ammonium sulfate, succinic acid, and the 50:50 ammonium sulfate/succinic acid system dried using a TB (phase-separated morphology) and DD (homogeneous morphology).

Dp_{50}. As a result of the difference when the averaging was performed, values for Dp_{50} can differ by 1−2 nm. Note that, while a slight difference is observed between the activation diameters of ammonium sulfate and the partially engulfed (TB) system, they are within experimental error. On the basis of the results of Rose et al., we expect that correcting for deviations from the theoretical transfer function will result in an equivalent activation diameter and an even steeper slope of the activation curve for phase-separated particles.[28]

For the 50:50 ammonium sulfate/succinic acid system, an activation diameter of Dp_{50} = 52 nm (σ_{est} = 5%) was obtained for phase-separated particles, while a homogeneous morphology resulted in a Dp_{50} = 55 nm (σ_{est} = 5%). Figure 5 summarizes the CCN spectra for ammonium sulfate, succinic acid, and the 50:50 ammonium sulfate/succinic acid system dried using a TB (phase-separated morphology) and DD (homogeneous morphology). Note again that, while a slight difference is observed between the activation diameters of ammonium sulfate and the partially engulfed (TB) system, they are within experimental error. On the basis of the results of Rose et al., we expect that correcting for deviations from the theoretical transfer function will result in an equivalent activation diameter and an even steeper slope of the activation curve for phase-separated particles.[28]

Surprisingly, the CCNC data for the 50:50 mixtures show that, given two systems of identical composition, particle morphology has a noticeable effect on the activation diameter. Thus, the efficiency of particles to serve as CCN changes between phase-separated and homogeneous morphologies. Specifically, the activation diameter of phase-separated particles is similar to that of ammonium sulfate for the systems studied in this work. As shown in our previous work, both pimelic acid and succinic acid mixtures with ammonium sulfate yield a partially engulfed morphology upon phase separation and drying.[13] Homogeneous particles, on the other hand, have an activation diameter that is in between the pure inorganic and organic components. On the basis of the Zdanovskii−Stokes−Robinson (ZSR) model, we would expect that the κ factors that are obtained for the homogeneous 50:50 mixtures would be equivalent to the volume-weighted average of the components, as shown by

$$\kappa_{\text{homogeneous}} = \frac{V_{\text{org}}}{V_{\text{tot}}}\kappa_{\text{org}} + \frac{V_{\text{inorg}}}{V_{\text{tot}}}\kappa_{\text{inorg}} \quad (2)$$

where V_{org}, V_{inorg}, and V_{tot} are the volumes of the organic component, inorganic component, and total, respectively, and κ_{org}, κ_{inorg}, and $\kappa_{homogeneous}$ are the κ values for the organic component, inorganic component, and homogeneous particle, respectively.[29] Because κ is related to diameter, the expected Dp_{50} for mixtures would similarly fall between that of the two component Dp_{50} values.

In contrast to the results for homogeneous particles, our results for phase-separated (partially engulfed) particles are surprising and additional studies will need to be performed to fully understand the origin of the results. To begin to explain the results for partially engulfed particles, we can consider the implications of this morphology on the Köhler curve, given by

$$s_k = \frac{2\sigma}{n_L R T r_d} - \frac{3iN_s}{4\pi n_L r_d^3} \quad (3)$$

where s_k is the supersaturation, σ is the surface tension, n_L is the number of moles of water in 1 L of solution, R is the ideal gas constant, T is the temperature, i is the van't Hoff factor, which accounts for the dissociation of salts into ions in solution, N_s is the total moles of solute, and r_d is the radius of the particle.[29] In a partially engulfed particle, water vapor has direct access to the ammonium sulfate component. With this morphology, it is likely that the water solvates ammonium sulfate prior to the less hygroscopic organic component. For the ammonium sulfate/pimelic acid system, it is a reasonable approximation that the pimelic acid is effectively insoluble when ammonium sulfate is at the point of activation based on the fact that the activation curves for ammonium sulfate and pimelic acid in Figure 4 have little overlap. At the point at which the particle activates, pimelic acid will therefore not influence the surface tension. As a result, the first term in eq 3 should remain the same as for an ammonium sulfate particle. The amount of soluble material has decreased (considering only the ammonium sulfate component), reducing the second term in eq 3. As a result, the supersaturation will increase, leading to an increase in the activation diameter. However, the pimelic acid also serves as a heterogeneous catalyst, which will decrease the activation barrier for activation, lowering the activation diameter.[30] For ammonium sulfate/succinic acid, a fraction of the succinic acid

DOI: 10.1021/acsearthspacechem.7b00146
ACS Earth Space Chem. 2018, 2, 634−639

particles are activated at the point at which 50% of the ammonium sulfate particles activate, as shown in Figure 5. For particles in which succinic acid is not activated, the case is the same for pimelic acid. Activation of some succinic acid particles may result in a decrease in surface tension. Surface partitioning of organic compounds impacts CCN activation and hygroscopic growth of organic aerosol.[5,31−35] Surface-active organics can affect cloud droplet formation by reducing surface tension and resulting in a larger size droplet at the point of activation.[5,31−35] These effects result in a reduced supersaturation and reduced activation diameter. From the above discussion, we can conclude that a partially engulfed particle likely activates at a smaller diameter than a homogeneous particle, but it is striking that the experimental result shows activation at approximately the same diameter as ammonium sulfate. Additional work needs to be performed to determine why this is the case. We also note that the presence of other morphologies (e.g., core−shell) may also impact CCN activation and will be explored in future studies.

An effect of LLPS on CCN activation has been previously reported by Ovadnevaite et al.[12] Bertram and co-workers determined that secondary organic material (SOM) can undergo LLPS without the presence of salt because the RH is increased to >90% as a result of the difference in solubility of the components of the SOM.[10,11] At a high RH, the less soluble components of SOM form a new phase at the surface of the particle, which lowers the surface tension of the aqueous particle. Ovadnevaite et al. hypothesize that the resultant reduction in surface tension leads to much greater numbers of CCN observed in the field than expected.[12] In contrast, aerosol used in this study is a combination of an organic compound and a salt, which undergo LLPS as the RH is decreased below a given value as a result of salting out of the organic compound.

CONCLUSIONS AND ATMOSPHERIC IMPLICATIONS

We have investigated the effect of particle morphology on CCN activity. Using our results from earlier work where a size-dependent morphology was observed for aerosol particles composed of organic compounds and salts, we have specifically studied the difference in activation caused by a homogeneous versus phase-separated morphology. Interestingly, for systems of identical composition, distinct morphologies lead to noticeable changes in CCN behavior. For 50:50 mixtures of ammonium sulfate/pimelic acid and ammonium sulfate/succinic acid, a phase-separated morphology results in activation diameters close to that of ammonium sulfate, while a homogeneous morphology yields an activation diameter in between the pure components. The data presented in this study indicate that morphology is an important parameter in determining CCN activity for the systems investigated in this work. By accurately assessing and accounting for the effect of morphology, cloud microphysics models will be able to better predict the CCN activity of mixed atmospheric particles containing complex organics. Furthermore, by combining particle composition information and morphology-resolved CCN data, we can compute hygroscopicity parameters for multicomponent aerosol particles containing varying amounts of inorganic and organic compounds. To better predict the impact of aerosol particles on cloud properties and the radiative balance of the Earth, our experiments suggest that it is important to investigate whether models should incorporate the complex physical and chemical parameters of aerosol particles that become CCN.

ASSOCIATED CONTENT

Supporting Information

The Supporting Information is available free of charge on the ACS Publications website at DOI: 10.1021/acsearthspacechem.7b00146.

Individual activation curves and fits for the internally mixed systems of ammonium sulfate/pimelic acid and ammonium sulfate/succinic acid (PDF)

AUTHOR INFORMATION

Corresponding Author

*Telephone: 814-867-4267. E-mail: maf43@psu.edu.

ORCID

Miriam Arak Freedman: 0000-0003-4374-6518

Notes

The authors declare no competing financial interest.

ACKNOWLEDGMENTS

The authors are grateful for support from the Faculty Early Career Development Program (CAREER) of the National Science Foundation (NSF) (CHE-1351383) for the collection of data and NSF Grants AGS-1723290 (to Muhammad Bilal Altaf and Miriam Arak Freedman) and AGS-1723874 (to Dabrina D. Dutcher and Timothy M. Raymond) for the analysis and interpretation.

REFERENCES

(1) Stocker, T. F.; Qin, D.; Plattner, G.-K.; Tignor, M. M. B.; Allen, S. K.; Boschung, J.; Nauels, A.; Xia, Y.; Bex, V.; Midgley, P. M. *Climate Change 2013: The Physical Science Basis: Contribution of Working Group I to the Fifth Assessment Report of the Intergovernmental Panel on Climate Change*; Cambridge University Press: Cambridge, U.K., 2013.

(2) Wallace, J. M.; Hobbs, P. V. *Atmospheric Science: An Introductory Survey*; Academic Press: London, U.K., 2006.

(3) Rose, D.; Gunthe, S. S.; Mikhailov, E.; Frank, G. P.; Dusek, U.; Andreae, M. O.; Pöschl, U. Calibration and measurement uncertainties of a continuous-flow cloud condensation nuclei counter (DMT-CCNC): CCN activation of ammonium sulfate and sodium chloride aerosol particles in theory and experiment. *Atmos. Chem. Phys.* **2008**, *8* (5), 1153−1179.

(4) Engelhart, G. J.; Asa-Awuku, A.; Nenes, A.; Pandis, S. N. CCN activity and droplet growth kinetics of fresh and aged monoterpene secondary organic aerosol. *Atmos. Chem. Phys.* **2008**, *8* (14), 3937−3949.

(5) Ruehl, C. R.; Davies, J. F.; Wilson, K. R. An interfacial mechanism for cloud droplet formation on organic aerosols. *Science* **2016**, *351* (6280), 1447−1450.

(6) Farmer, D. K.; Cappa, C. D.; Kreidenweis, S. M. Atmospheric Processes and Their Controlling Influence on Cloud Condensation Nuclei Activity. *Chem. Rev.* **2015**, *115* (10), 4199−4217.

(7) Slade, J. H.; Shiraiwa, M.; Arangio, A.; Su, H.; Pöschl, U.; Wang, J.; Knopf, D. A. Cloud droplet activation through oxidation of organic aerosol influenced by temperature and particle phase state. *Geophys. Res. Lett.* **2017**, *44* (3), 1583−1591.

(8) Rastak, N.; et al. Microphysical explanation of the RH-dependent water affinity of biogenic organic aerosol and its importance for climate. *Geophys. Res. Lett.* **2017**, *44* (10), 5167−5177.

(9) Hodas, N.; Zuend, A.; Schilling, K.; Berkemeier, T.; Shiraiwa, M.; Flagan, R. C.; Seinfeld, J. H. Discontinuities in hygroscopic growth below and above water saturation for laboratory surrogates of oligomers in organic atmospheric aerosols. *Atmos. Chem. Phys.* **2016**, *16*, 12767−12792.

DOI: 10.1021/acsearthspacechem.7b00146
ACS Earth Space Chem. 2018, 2, 634−639

(10) Renbaum-Wolff, L.; Song, M.; Marcolli, C.; Zhang, Y.; Liu, P. F.; Grayson, J. W.; Geiger, F. M.; Martin, S. T.; Bertram, A. K. Observations and implications of liquid−liquid phase separation at high relative humidities in secondary organic material produced by α-pinene ozonolysis without inorganic salts. *Atmos. Chem. Phys.* **2016**, *16*, 7969−7979.
(11) Song, M.; Liu, P.; Martin, S. T.; Bertram, A. K. Liquid-liquid phase separation in particles containing secondary organic material free of inorganic salts. *Atmos. Chem. Phys.* **2017**, *17*, 11261−11271.
(12) Ovadnevaite, J.; et al. Surface tension prevails over solute effect in organic-influenced cloud droplet activation. *Nature* **2017**, *546* (7660), 637−641.
(13) Veghte, D. P.; Altaf, M. B.; Freedman, M. A. Size Dependence of the Structure of Organic Aerosol. *J. Am. Chem. Soc.* **2013**, *135* (43), 16046−16049.
(14) Altaf, M. B.; Freedman, M. A. Effect of Drying Rate on Aerosol Particle Morphology. *J. Phys. Chem. Lett.* **2017**, *8*, 3613−3618.
(15) Altaf, M. B.; Zuend, A.; Freedman, M. A. Role of nucleation mechanism on the size dependent morphology of organic aerosol. *Chem. Commun.* **2016**, *52* (59), 9220−9223.
(16) Veghte, D. P.; Bittner, D. R.; Freedman, M. A. Cryo-transmission electron microscopy imaging of the morphology of submicron aerosol containing organic acids and ammonium sulfate. *Anal. Chem.* **2014**, *86*, 2436−2442.
(17) Stolzenburg, M. R. An Ultrafine Aerosol Size Distribution Measuring System. Ph.D. Thesis, University of Minnesota, Minneapolis, MN, 1988.
(18) Stolzenburg, M. R.; McMurry, P. H. An Ultrafine Aerosol Condensation Nucleus Counter. *Aerosol Sci. Technol.* **2008**, *42*, 421−432.
(19) Veghte, D. P.; Freedman, M. A. The Necessity of Microscopy to Characterize the Optical Properties of Size-Selected, Nonspherical Aerosol Particles. *Anal. Chem.* **2012**, *84*, 9101−9108.
(20) Veghte, D. P.; Moore, J. E.; Jensen, L.; Freedman, M. A. Influence of shape on the optical properties of hematite aerosol. *J. Geophys. Res.: Atmos.* **2015**, *120*, 7025−7039.
(21) Veghte, D. P.; Altaf, M. B.; Haines, J. D.; Freedman, M. A. Optical Properties of Non-Absorbing Mineral Dust Components and Mixtures. *Aerosol Sci. Technol.* **2016**, *50*, 1239.
(22) Roberts, G. C.; Nenes, A. A Continuous-Flow Streamwise Thermal-Gradient CCN Chamber for Atmospheric Measurements. *Aerosol Sci. Technol.* **2005**, *39* (3), 206−221.
(23) Wiedensohler, A.; Lütkemeier, E.; Feldpausch, M.; Helsper, C. Investigation of the bipolar charge distribution at various gas conditions. *J. Aerosol Sci.* **1986**, *17*, 413−416.
(24) Petters, M. D.; Prenni, A. J.; Kreidenweis, S. M.; DeMott, P. J. On measuring the critical diameter of cloud condensation nuclei using mobility selected aerosol. *Aerosol Sci. Technol.* **2007**, *41*, 907−913.
(25) Weingartner, E.; Gysel, M.; Baltensperger, U. Hygroscopicity of Aerosol Particles at Low Temperatures. 1. New Low-Temperature H-TDMA Instrument: Setup and First Applications. *Environ. Sci. Technol.* **2002**, *36* (1), 55−62.
(26) Topping, D. O.; Mcfiggans, G. B.; Coe, H. A curved multi-component aerosol hygroscopicity model framework: Part 1—Inorganic compounds. *Atmos. Chem. Phys.* **2005**, *5* (5), 1205−1222.
(27) Petters, M. D.; Kreidenweis, S. M. A single parameter representation of hygroscopic growth and cloud condensation nucleus activity. *Atmos. Chem. Phys.* **2007**, *7* (8), 1961−1971.
(28) Rose, D.; Gunthe, S. S.; Mikhailov, E.; Frank, G. P.; Dusek, U.; Andreae, M. O.; Pöschl, U. Calibration and measurement uncertainties of a continuous-flow cloud condensation nuclei counter (DMT-CCNC): CCN activation of ammonium sulfate and sodium chloride aerosol particles in theory and experiment. *Atmos. Chem. Phys.* **2008**, *8*, 1153−1179.
(29) Seinfeld, J. H.; Pandis, S. N. *Atmospheric Chemistry and Physics: From Air Pollution to Climate Change*, 2nd ed.; Wiley: Hoboken, NJ, 2006.
(30) Lamb, D.; Verlinde, J. *Physics and Chemistry of Clouds*; Cambridge University Press: New York, 2011.
(31) Werner, J.; Dalirian, M.; Walz, M.-M.; Ekholm, V.; Wideqvist, U.; Lowe, S. J.; Öhrwall, G.; Persson, I.; Riipinen, I.; Björneholm, O. Surface Partitioning in Organic−Inorganic Mixtures Contributes to the Size-Dependence of the Phase-State of Atmospheric Nanoparticles. *Environ. Sci. Technol.* **2016**, *50* (14), 7434−7442.
(32) Vanhanen, J.; Hyvärinen, A.-P.; Anttila, T.; Raatikainen, T.; Viisanen, Y.; Lihavainen, H. Ternary solution of sodium chloride, succinic acid and water; surface tension and its influence on cloud droplet activation. *Atmos. Chem. Phys.* **2008**, *8* (16), 4595−4604.
(33) Prisle, N. L.; Dal Maso, M.; Kokkola, H. A simple representation of surface active organic aerosol in cloud droplet formation. *Atmos. Chem. Phys.* **2011**, *11* (9), 4073−4083.
(34) Blower, P. G.; Ota, S. T.; Valley, N. A.; Wood, S. R.; Richmond, G. L. Sink or Surf: Atmospheric Implications for Succinic Acid at Aqueous Surfaces. *J. Phys. Chem. A* **2013**, *117* (33), 7887−7903.
(35) *Atmospheric and Aerosol Chemistry*; McNeill, V. F., Ariya, P. A., Eds.; Springer: Berlin, Germany, 2014; Topics in Current Chemistry, Vol. *339*, DOI: 10.1007/978-3-642-41215-8.

DOI: 10.1021/acsearthspacechem.7b00146
ACS Earth Space Chem. 2018, 2, 634−639